Earth, Moon, and Planets (2004) 95: 265–277
DOI 10.1007/s11038-005-9031-0

VIDEO AND PHOTOGRAPHIC SPECTROSCOPY OF 1998 AND 2001 LEONID PERSISTENT TRAINS FROM 300 TO 930 nm

SHINSUKE ABE
Astronomical Institute of the Academy of Sciences, Ondrejov, 25165 The Czech Republic (E-mail: avell@asu.cas.cz)

NOBORU EBIZUKA
RIKEN (The Institute of Physical and Chemical Research), Wako, 351-0198 Saitama, Japan

HIDEYUKI MURAYAMA, KATSUHITO OHTSUKA
Tokyo Meteor Network, 1-27-5 Daisawa, Setagaya, 155-0032 Tokyo, Japan

SATORU SUGIMOTO
Tochigi Astronomical Group, 1958-4 Tsurutamachi, Utsunomiya, 320-0851 Tochigi, Japan

MASA-YUKI YAMAMOTO
Kochi University of Technology, 185 Miyanokuchi, Tosayamada, 782-8502 Kochi, Japan

HAJIME YANO
Institute of Space and Astronautical Science, Japan Aerospace Exploration Agency, 3-1-1 Yoshinodai, Sagamihara, 229-8510 Kanagawa, Japan

JUN-ICHI WATANABE
National Astronomical Observatory of Japan, National Institutes of Natural Sciences, 2-21-1 Osawa, Mitaka, 181-8588 Tokyo, Japan

JIŘÍ BOROVIČKA
Astronomical Institute of the Academy of Sciences, Ondrejov, 25165 The Czech Republic

(Received 15 November 2004; Accepted 30 May 2005)

Abstract. Spectra of persistent meteor trains were observed at wavelength between 300 and 930 nm. Two obtained train spectra during the 1998 and 2001 Leonid meteor showers are reported here. During the 1998 Leonids, one train was detected by a photographic camera with a spectrograph covering 370–640 nm region. On the other hand, during the 2001 Leonids, video observations were carried out using image intensified cameras in ultraviolet (UV), visible and near infrared (near-IR) wavelengths. Temperatures in persistent trains have been measured by atmospheric O_2 A(0,1) band at the wavelength near 864.5 nm. From a video spectrum obtained just 7 s after parent fireball's flare, a rotational temperature of 250 K at altitude of 88.0 ± 0.5 km was estimated. We can say that the cooling time scale of train strongly depends on the initial mass of its fireball at least for Leonids. Based on cooling constant calculated from our results, we estimated a temperature of ~130 K as a final exothermic temperature at early stage of persistent trains.

Keywords: Airglow, Leonid meteor shower, meteors, persistent train, astrobiology

1. Introduction

Bright fireballs sometimes leave a long-lasting glow that is called a persistent train which lasts long after the disappearance of its parent meteor. It is evident that short lasting trains called a short duration train, which last several seconds at the most, emit a forbidden line of [O I] at 557.7 nm (Halliday, 1958; Millman, 1962) known as the aurora green line. After a rapid decay in intensity, it is generally believed that the luminosity of persistent trains is fueled by reactions involving O_3 and atomic O, efficiently catalyzed by metals from the freshly ablated meteoroids.

Von Konkoly was the first man who carried out a spectroscopic observation of a persistent train by a direct vision spectroscope in 1873 (Herschel, 1881). Afterwards, low resolution photographic spectra of persistent trains were obtained, i.e., six spectra at Banska Bystrica Observatory, Slovakia, observed in 1986–1993 (Rajchl and Peresty, 1992), four spectra in Japan during the 1993 Perseid maximum (Rajchl et al., 1995) and two spectra of the 1993 Perseids in Slovakia (Borovička et al., 1996). All these spectra have shown two main emissions; multiplets of MgI at 518 nm and NaI at 589 nm. The Leonid meteors tend to leave long-lasting persistent trains because of its high entry velocity, ~71 km/s. The parent comet, 55P/Tempel-Tuttle, has an orbital period of 33 years, passed perihelion on February 28, 1998. Therefore, after 1998, the Leonid meteor showers brought us epoch-making observations for persistent trains year by year (Borovička and Jenniskens, 2000; Chu et al., 2000; Jenniskens et al., 2000b; Kelley et al., 2000; Drummond et al., 2001., Abe et al., 2003; Suzuki, 2003). Although the persistent trains has been an object of study for a long time, the physical process of trains is still far from satisfactory. The main reason is that the number of spectrum of persistent train is still lacking and spectrum in the wide wavelength ranges are also still absent. Moreover, spectrum of the persistent trains were obtained only by means of slitless spectrographs which cannot identify molecular emissions precisely. Plane (2003) provides a summary of atmospheric chemistry of meteoric metals.

This paper is intended as an investigation of an early stage of persistent train based on photographic and video spectroscopy with slitless spectrographs in the extensive range between 300 and 930 nm.

2. Observations

We report here slitless spectroscopic observations of persistent meteor trains performed with a photographic camera during the 1998 Leonids and two

image intensified video cameras during the 2001 Leonids. Figure 1 shows sensitivity curves combined with three different spectroscopic instruments. The coverage wavelength was between 300 and 930 nm. The data shown here is based on the analysis of two excellent persistent trains. The first (TR98) and second (TR01) spectrum were obtained in 1998 and 2001, respectively. For photographic results (TR98), we have precise orbital data of the parent meteor and the estimated error of altitude is within ± 0.2 km. While for video results (TR01), orbital information on the parent meteor didn't exist, thus we performed by using several train images observed from different places. Finally, the estimated error of altitude is about ± 0.5 km which depends on the total number of triangulation images. In the following, we defined the time '$t=0$' as the brightest moment of meteor flare and the time precisions are ± 0.5 s for photographic spectra (TR98) and ± 0.03 s for video spectra (TR01).

2.1. Photographic observation of the 1998 leonid meteor train

The photographic observations were carried out using a 35 mm size photographic camera with a grating of 300 grooves/mm, blazed wavelength of 490 nm. The camera was used with an $f=85$ mm, F/1.2 lens and a panchromatic film Kodak T-MAX-400. The observational site was about 20 km east of Nobeyama Radio Observatory of National Astronomical Observatory of Japan (138°.47 E, +36°.03 N, 1150 m). The effective spectral region

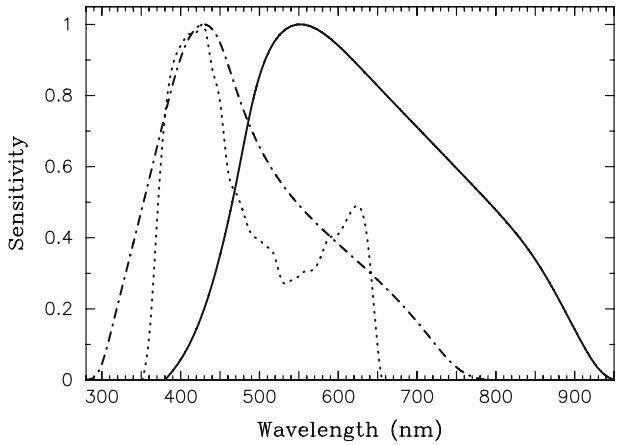

Figure 1. Combined with effective spectral sensitivity responses of three distinguished instruments. The sensitivities were constructed by measuring spectra of bright stars mainly in the observing field and were normalized at its maximum. These sensitivity covered the wavelength at 370–640 nm for photographic (dotted curve), 400–930 nm for the ICCD (thick curve) and 300–750 nm for the UV-II-HDTV (broken curve).

was the wavelength of 370–640 nm. In order to prevent blending of the 1st and the 2nd order image, we used a filter (Kenko L37) which cut off sharply below 350 nm and transmissibility of 50% at 370 nm. One Leonid fireball of which estimated magnitude was −8 appeared at 19:13:55 UT on November 17, 1998. This meteor left a persistent train which was visible by the naked eye for more than 15 min. A 10 s exposure was started from 12 s after the fireball disappearance.

The photographs were digitized with 1024 intensity levels. Dark frame subtracting and flat-fielding were applied to the digital images. A deconvolution method by using a spread function of the persistent train was applied to derive an undisturbed spectrum under an ideal condition because the image showed spreadable distribution caused by the strong upper atmospheric wind within rather long exposure time of 10 s. The spectroscopic image of the persistent train is shown in Figure 2. An analyzed train spectrum with identifications at the altitude of 87.0 ± 0.2 km is shown in Figure 3.

2.2. Video observation of the 2001 leonid meteor train

Here we report wonderful persistent spectra related with a Leonid meteor fireball, which were observed from two stations at 16:47:24 UT on November 18, 2001. A strong meteor storm activity was well observed around 18:16 UT with the zenithal hourly rate of 3730 caused by a dust trail ejected from comet 55P/Tempel-Tuttle in 1866 McNaught and Asher (1999). Because the physical environment including temperature and density should have changed with time, it would be better to take shorter exposure time. From two stations, spectra were recorded in NTSC video rate, 30 frames per second, and from both stations, the train spectra were obtained just 7 s after meteor flare, the brightest part of the parent fireball which was approximately −8 magnitude.

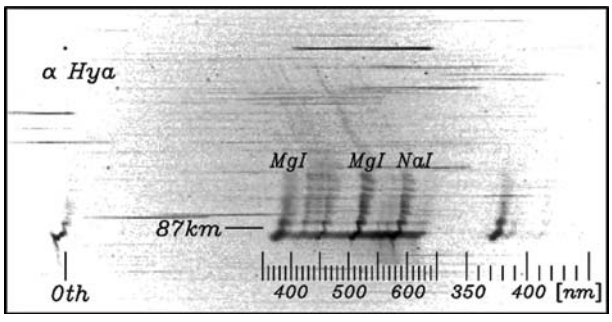

Figure 2. Photographic spectrum of TR98 with an exposure time of 10 s. The dispersion direction is from left to right and the fireball moved from top to bottom. The 0th, the 1st and a part of the 2nd order images were observed.

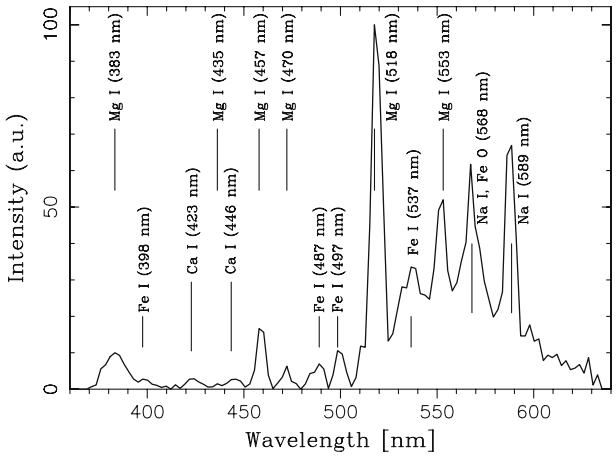

Figure 3. Spectral identifications of TR98 at the height of 87.0 ± 0.2 km, $t = 12-22$ s. The intensity calibrated by sensitivity response is normalized to 100 at MgI (518 nm). Iron lines are indicated on the extreme down without the atomic name.

2.2.1. *ICCD: visible and near-infrared region (400–930 nm)*
The observation was done in Tochigi prefecture (140°.05 E, 37°.09 N, 580 m). The ICCD system consisted of a 150 grooves/mm objective gratings, blazed at 575 nm and a second generation image intensifier (Hamamatsu Photonics, ϕ28 mm Night Viewer C3100) which was performed with an $f = 85$ mm, F/1.2 lens. This system provided a circular field of view of 26° in diameter. The spectrum was recorded by NTSC standard digital video camera (SONY PC-3). For taking morphology of persistent trains, the same ICCD system without spectrographs was used on the same observational mount simultaneously. The observing mount had three axes, azimuth, elevation and radiant axes. Once the radiant axis was set to the direction of a radiant of meteor shower, the spectroscopic dispersion direction in the field of view always turned on perpendicular to the meteor path automatically. This special mount takes advantage of unexpected phenomena such as persistent trains because the faster pointing is better and more important for train's spectroscopy. All analyzed spectrum were obtained by averaging of 30 video frames (duration of 1 s) to reduce the noise of the image intensifier. An example of spectroscopic image of the persistent train is shown in Figure 4.

2.2.2. *UV-II-HDTV: ultraviolet and visible region (300–600 nm)*
Ozone in the stratosphere strongly absorbs below 290 nm, preventing the UV light from reaching the Earth's surface. In order to prevent air extinction owing to mainly aerosol scattering in the UV wavelength below 380 nm, the

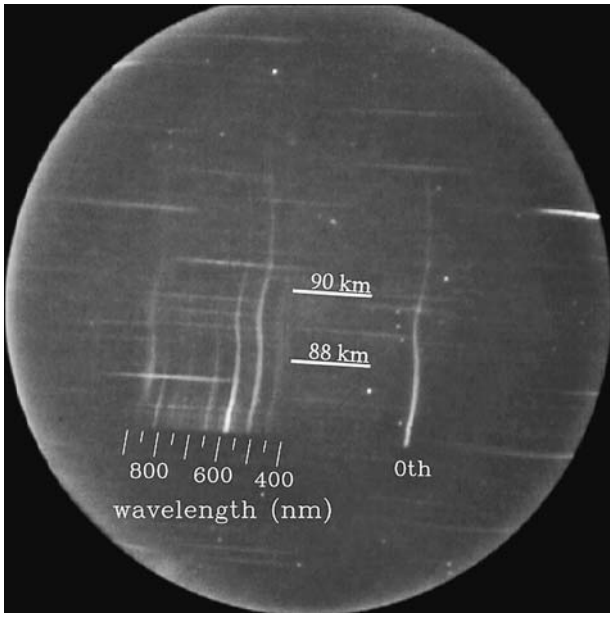

Figure 4. Video spectrum of TR01 by averaging of 1 s (30 frames) before flat-fielding and subtracting of dark and bias. The dispersion direction is from right to left and the fireball moved from top to bottom.

spectroscopic observation was performed at a high-altitude site in the Nobeyama Radio Observatory of National Astronomical Observatory of Japan. The video observations were carried out using an Image-Intensified High Definition TV (II-HDTV) camera in the ultraviolet, visible and near-infrared wavelength regions (250–700 nm). The UV-II-HDTV system consisted of an orginal uv lens ($f = 30$ mm, F/1.2), a UV image intensifier (ϕ 18 mm photocathode: S20), two relay lenses ($f = 50$ mm, F/1.4), and an HDTV camera with and objective sprectrometer of a 2 mega pixels CCD. Spectroscopic observations were performed by the UV-II-HDTV system equipped with an objective spectometer of a reflection grating, which is 600 grooves/mm, blazed at 330 nm, manufactured by the Richardson Grating Laboratory. The rectangular field of view was $23° \times 13°$ in diameter and spectral resolution FWHM = 2.5 nm in the first order. Since no order-sorting filter was used, it turns out that the first-order spectrum was mixed with the second-order spectrum in the wavelength longer than 600 nm. The first results of the II-HDTV spectrum obtained from 1999 Leonids and the first results of the UV-II-HDTV spectrum were described in Abe et al. (2000), Abe et al. (2000), and Abe et al. (2005).

From these simultaneous observation in UV and visible region (300–930 nm), an extensive combined spectrum is shown in Figure 5. The identifications of significant compositions are summarized in Table I.

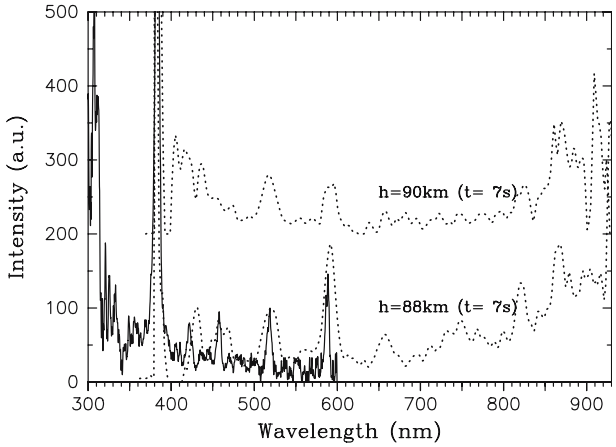

Figure 5. 300–900 nm combined spectrum of TR01 at the height of 88 ± 0.5 km and 90 ± 0.5 km (shifted to upper by 200), $t = 7 - 8$ s. Train spectra were observed by the ICCD (400–930 nm: dotted curve) and the UV-II-HDTV (300–600 nm: thick curve) simultaneously. The intensities calibrated by sensitivity responses are normalized to 100 at MgI (518 nm).

2.3. Triangulation observations of persistent trains

The MEteor TRain Observation (METRO) campaign was widely announced to amateur observers in Japan since the 1998 Leonids and resulted in great success for triangulation observations (Toda et al., 2004; Higa et al., 2005). During the 1998–2001 Leonids over Japan, 173 persistent trains including 53 triangulations were reported with the aid of photographs and video recordings. All these efforts made it clear that the probability of appearance of persistent train was approximately 20% for all Leonid fireballs brighter than −2 magnitude and long-lived trains tended to remain at the altitude between 85.8 and 98.5 km (Yamamoto et al., 2005). The triangulation data provided from METRO campaign enabled us to calculate three-dimensional structure of trains with its precise height information.

3. Results and Discussion

According to the analysis of 8 cases of persistent trains related with Leonid meteoroids, we recognized that continuum dominated emission, so called the molecular phase, begins between 30 and 40 s after meteor disappearance. In the following, we shall focus on an early stage of persistent trains, named the atomic phase, for understanding its physical conditions, that will lead to understand the molecular phase in the future work.

TABLE I
Identifications of Train Spectra of TR98 and TR01. Intensities are normalized to 100 at MgI (518 nm)

λ_{obs} nm	Int. a.u.	λ_{lab}	composition	λ_{obs}	Int. a.u.	λ_{lab}	composition
307.4	554	307.0	OH(A–X)	457.6	95	457.1	MgI
		307.5	FeI	469.8	39	470.3	MgI
309.6	365	309.0	OH(A–X)	478.8	37	478.3	MnI
		309.3	MgI	487.0	32	487.1	FeI
		309.7	MgI	496.4	39	496.6	FeI
310.6	387	310.7	OH(A–X)	516.2	74	515.3	NaI
312.0	385	311.9	FeI	518.8	100	516.7	MgI
320.8	188	320.2	MgI			517.3	MgI
325.8	144	325.8	FeI			518.4	MgI
333.0	131	333.2	MgI	537.4	33	537.1	FeI
		333.7	MgI	553.4	32	552.8	MgI
343.8	51	343.7	NiI	566.6	33		FeO
		344.1	FeI	569.4	33	568.3	NaI
348.8	89	349.1	FeI	586.4	117		FeO
355.8	88	355.9	FeI	588.6	146	589.0	NaI
359.6	80	359.3	CrI	612.3	36	612.2	CaI
		359.8	NiI	620.7	32	620.1	CaI
363.2	66	363.1	FeI	631.2	30	631.9	MgI
368.4	84	368.3	FeI	656.4	65	657.3	CaI
369.6	84	369.5	FeI	673.2	36	672.2	SiI
375.6	146	375.8	FeI			674.2	SiI
382.8	906	382.9	MgI	694.2	36	693.9	KI
		383.2	MgI	713.1	49	714.8	CaI
		383.8	MgI	732.0	70	732.6	CaI
390.0	104	390.0	FeI	746.7	84	746.8	NI
393.2	76	393.0	FeI	767.7	72	766.5	KI
		393.4	CaI	776.1	61	777	OI
397.6	57	397.8	FeI	788.7	55	788.2	MgI
404.6	51	404.6	FeI	799.2	69	797.6	SiI
406.2	53	406.4	FeI			802.7	SiI
410.6	54	410.3	SiI	820.2	134	818.3	NaI
		410.7	FeI			819.5	NaI
421.8	80	421.6	FeI	843.3	95	844.6	OI
422.8	72	422.7	CaI	853.8	100	855.7	SiI
425.0	56	425.1	FeI	862.6	175	863	O_2
434.8	43	434.5	CrI	866.4	187	866	O_2
		435.2	CrI	879.0	149	880.7	MgI
		435.2	MgI	895.8	150	894.9	SiI

TABLE I (Continued)

λ_{obs} nm	Int. a.u.	λ_{lab}	composition	λ_{obs}	Int. a.u.	λ_{lab}	composition
443.2	44	443.1	FeI	904.2	153	902.2	SiI
		443.5	CaI	916.8	147	915.4	NaI
446.0	47	445.5	CaI				
		445.9	FeI				
		446.2	FeI				

To begin with, let us consider the emission energy contribution in the persistent train from UV to near-IR wavelength region. Since the UV-II-HDTV spectrum of TR01 was almost comparable to the ICCD spectrum of the same train in the overlapped region between 400 and 600 nm, the intensity ratios were derived from a combined spectrum which was generated by UV–visible and visible–near-IR spectrum after normalization at MgI (518 nm). Ratios of (300–400 nm)/(400–600 nm) = 2.5 from the UV-II-HDTV spectrum and (300–600 nm)/(600–900 nm) = 1.0 from both UV-II-HDTV and ICCD spectra were estimated. It is also important to note that at the lower altitude, 88.0 ± 0.5 km, of the train, NaI (589 nm) was stronger than MgI (518 nm) and was almost comparable to $O_2(0,1)$(~865 nm) (Figure 5: lower dotted curve), on the contrary, MgI and $O_2(0,1)$ were stronger than NaI in the upper altitude, 90.0 ± 0.5 km (Figure 5: upper dotted curve). In addition to this, there are remarkable differences in the spectra shown in Figures 3 and 5, in particular for the ratio of intensities of MgI at 518–383 nm, and existence and non-existence of continuum emission in 530–630 nm. These differences resulted from, (i)time-lag of beginning of exposure after the meteor disappearance, 7 s for TR01 in Figure 5 and 12 s for TR98 in Figure 3, and then the intensity of MgI (383 nm) showed much more stronger than that of MgI (518 nm) at the earlier stage, (ii)exposure time, 1 s for TR01 in Figure 5 and 10 s for TR98 in Figure 3, and then both the atomic and the molecular phase were included in TR98 (Figure 3).

Assuming that the atomic phase persistent train is in local thermodynamic equilibrium (LTE), an excitation temperature of ~2000 K was estimated from our results. However, The train temperature was expected to be lower than 1000 K. Because the density in the train was so low that thermal collisions which were required for LTE should be insufficient, we have to deal with non-equilibrium state. Borovička and Koten (2003) proposed that atomic recombination followed by electron downward cascade was responsible for the population of high levels and this process was a likely mechanism to produce the atomic phase of the train. In this case, the LTE temperature is not appropriate. It is worth while to notice that the equilibrium state of a molecular oxygen band $(b^1\Sigma_g^+) \longrightarrow (X^3\Sigma_g^-)$ takes advantage of dealing with

physical conditions in persistent trains while atomic lines are under non-equilibrium conditions.

Baggaley (1976) strongly suggested that characteristics of the red train was responsible for an excited atmospheric molecular oxygen, O_2 A(0,1) ($b^1\Sigma_g^+$ state) (hereafter O_2 (0,1)) first identified in the nightglow by meinel (1950). The presence of the molecular oxygen in a persistent train was first suspected by Hapgood (1980). He reported the enhancement of near-IR emission with the aid of an image isocon television camera which sensitivity covered at 700–900 nm. Long afterwards, Clemesha et al. (2001) also detected O_2 (0,1) by means of CCD imaging with a 12 nm bandpass filter. Finally, Suzuki (2003) first identified O_2 (0,1) band from several persistent trains which was carried out by a high resolution CCD spectroscopy with 5 s exposure time. Because another vibrational band of O_2 (0,0) at 761.9 nm is absorbed by the lower lying atmospheric O_2 and consequently not observed from the ground, (0,1) is the strongest O_2 atmospheric band with the emission origin at 864.5 nm and *P* and *R* branches having maxima around 866 and 863 nm, respectively, that center wavelength slightly depends on excited temperature. Although spectral resolution in our video observation was low, ~2 nm, *P* and *R* branches were confirmed separately. The O_2 (0,1) showed its strongest intensity at the altitude of 88.0 and lasted until ~14 s after meteor flare. Figure 6 indicates comparison between synthetic spectra of O_2 (0,1) at appropriate rotational temperatures (100–300 K) and observed spectra. The temperature dependency of the band structure can be seen clearly in the observed train spectra. The train spectra at the altitude of 88.0 km obtained just 7 s after flare is almost in complete agreement with the model spectrum calculated by the rotational temperature of 250 K. Some other (un-identified)

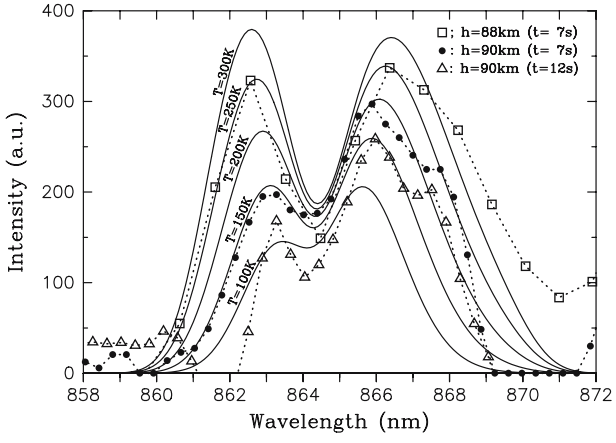

Figure 6. Comparison between synthetic spectra of O_2 A(0,1) at appropriate rotational temperatures (100–300 K) and observed spectra at the altitude of 88.0 and 90.0 km. The intensities of *P* and *R* branches of O_2 emission vary with the rotational temperature.

emission lines may be blended with the pure O_2 (0,1) band beyond 866 nm, or the longer wavelength near the edge of the sensitivity caused a little calibration error. The temperature at the altitude of 90.0 km shows about 150–200 K, which is slightly lower than that of 88.0 km. A temperature of the observed spectrum just 12 s after flare at the altitude of 88.0 km was ~150 K. A standard atmospheric temperature at 90.0 km altitude represented by the U.S. Standard Atmosphere (USSA 1976) is 187 K. Chu et al. (2000) reported from lidar observations of a double-tube-structured persistent train that approximately 3 min after ablation, Na temperatures of about 230 K at 92.2 km altitude and 260 K at 92.35 km altitude are compared with our results of O_2 (0,1) rotational temperature of 250 K, even though the time passage was different. Temperature decay curves up to 2 s were reported from −3 to −13 fireball (Jenniskens and Mandell, 2004a). Our results occurred from −8 magnitude fireball can be explained between these two decay curves extrapolated to 7 and 12 s. It seems reasonable to suppose that the cooling time scale of a train depends on the initial mass of its fireball.

During *the afterglow phase*, Borovička and Jenniskens (2000) found that the decay of line intensities depends on excitation potential, not on transition probability. The decay is therefore due primarily to the decrease of temperature, not density. The next equation was found: $5040/T(t) = 5040/T(0) - Dt$. In the case of *the afterglow phase*, the temperature decreased from $T(0) = 4500$ K, typical temperature of Leonid meteors, to $T(2.7) = 1000$ K within 2.7 s and the value of the cooling constant D was found to be $D \sim -1.5$. We adopted this equation to the case of *the atomic phase* of TR01 spectra at $t = 7$ s($T(7) = 250$ K) and 12 s($T(12) = 150$ K), respectively. Finally, the same $D \sim -2.7$ was measured from both spectra at $t = 7$ and 12 s. It therefore seems that the above equation is valid for times up to 12 s. The cooling was quicker in this train than in that studied by borovička and Jenniskens (2000), which was caused by a brighter fireball. The O_2 emission faded away after 14 s in our spectrum. Though P and R branches were not seen clearly due to faint signal at $t = 14$ s, we speculate that after O_2 temperature decreased to ~130 K ($t = 14$ s), the exothermic emission was probably declining sharply and the O_2 emission must have disappeared.

Identified emissions in UV, visible, and near-IR ranges in the trains are completely different from Leonid fireballs observed by Abe et al. (2000), Abe et al. (2005), and Trigo-Rodriguez et al. (2004) . Of particular interest is the identification of molecular OH emitted in UV region around 310 nm. By means of the same instrument, the same OH feature was identified in a Leonid fireball spectrum (Abe et al. 2005). Further explanations of this emissions must be investigated. Meteors represent a unique chemical pathway towards prebiotic compounds on the early Earth (Jenniskens et al. 2000a, Jenniskens and Mandell 2004b). Because meteor persistent trains could emit in quite low temperature, less than 250 K, a significant fraction of

organic matter is expected to survive after fragmentation from a meteoroid. A long-lasting meteor train will provide us with good opportunities to investigate prebiotic molecules in the future work.

In this paper, we have been focused on *the atomic phase* of persistent trains especially for its emitters in multiple wavelength and induced temperatures resulted from $O_2(0,1)$. On the basis of these results, we are now ready to consider the long-lasting mechanism of *the molecular phase*. However, much still remains to be done in the forthcoming paper.

Acknowledgements

Special thanks are due to M. Toda and Y. Higa (NMS/METRO) for providing us triangulation images of persistent trains. The authors would like to thank M. Inoue (Nobeyama Radio Observatory, NAOJ/NINS) for their observational support. This research was supported by the National Astronomical Observatory of Japan of National Institutes of Natural Sciences, the Institute of Space and Astronautical Science of Japan Aerospace Exploration Agency, RIKEN (the Institute of Physical and Chemical Research), and the National Institute of Information and Communications Technology. This study is carried out as a part of "Ground-based Research Announcement for Space Utilization" promoted by Japan Space Forum. S.A. is supported by JSPS Postdoctoral Fellowships for Research Abroad.

References

Abe, S., Yano, H., Ebizuka, N., and Watanabe, J.-I.: 2000, *Earth, Moon, Planets* **8283**, 369–377.

Abe, S., Yano, H., Ebizuka, N., Kasuga, T., Sugimoto, M., and Watanabe, J.-I.: 2003, in H. Yano, S. Abe and M. Yoshikawa (eds.), *Proceedings of the 2002 International Science Symposium on the Leonid Meteor Storms*. Tokyo Press CO., LTD., pp. 149–157.

Abe, S., Ebizuka, N., Yano, H., Watanabe, J.-I., and Borovička, J.: 2005, *Astrophys. J.* **618**, L141–L144.

Baggaley, W. J.: 1976, *Bull. Astron. Inst. Czech.* **28**, 356–359.

Borovička, J. and Jenniskens, P.: 2000, *Earth, Moon, Planets* **8283**, 399–428.

Borovička, J. and Koten, P.: 2003, in H. Yano, S. Abe and M. Yoshikawa (eds.), *Proceedings of the 2002 International Science Symposium on the Leonid Meteor Storms*. Tokyo Press CO., LTD., pp. 165–173.

Borovička, J., Zimnikoval, P., Skvarka, J., Rajchl, J., and Spurny, P.: 1996, *Astron. Astrophys.* **306**, 995–998.

Chu, X. Z., Liu, A. Z., Papen, G., Gardner, C. S., Kelley, M., Drummond, J., and Fugate, R.: 2000, *Geophys. Res. Lett.* **27**, 1815–1818.

Clemesha, B. R., de Medeiros, A. F., Gobbi, D., Takahashi, H., Batista, P. P., and Taylor, M. J. J.: 2001, *Geophys. Res.* **28**, 2779–2782.

Drummond, J. D., Grime, B. W., Gardner, C. S., Liu, A. Z., Chu, X., and Kane, T. J. J.: 2001, *Geophys. Res.* **106**, 21517–21524.
Halliday, I.: 1958, *Astrophys. J.* **128**, 441–443.
Hapgood, M. A.: 1980, *Nature* **286**, 582–583.
Herschel, A. S.: 1881, *Nature* **29**, 507.
Higa Y., Toda M., Yamamoto M.-Y., and Watanabe J.-I.: 2005, *Publ. Natl. Astron. Obs. Japan* **7**, 67–141.
Jenniskens, P. and Mandell, A. M.: 2004a, *Astrobiology* **4**, 123–134.
Jenniskens, P. and Mandell, A. M.: 2004b, *Astrobiology* **4**, 95–108.
Jenniskens, P., Wilson, M. A., Packan, D., Laux, C. O., Boyd, I. D., Popova, O. P., and Fonda, M.: 2000a, *Earth, Moon, Planets* **82**(83), 57–70.
Jenniskens, P., Lacey, M., Allan, B. J., Self, D. E., and Plane, J. M. C.: 2000b, *Earth Moon Planets* **82**(83), 429–438.
Kelley, M. C., Gardner, C., Drummond, J. D., Armstrong, T., Liu, A., Chu, X., Papen, G., Kruschwitz, C., Loughmiller, P., Grime, B., and Engelman, J. J.: 2000, *Geophys. Res.* **13**, 1811–1814.
McNaught, R. H. and Asher, D. J.: 1999, *WGN J. Int. Meteor. Org.* **27**, 85–102.
Meinel, A. B.: 1950, *Astrophys. J.* **112**, 464–468.
Millman, P. M. J.: 1962, *RAS. Canada* **56**, 263–267.
Plane, J. M. C.: 2003, *Chem. Rev.* **103**, 4963–4984.
Rajchl, J. and Peresty, R.: 1992, *Astr. Inst. Czechosl. Acad. Sci.* **138**, 1–5.
Rajchl, J., Bocek, J., Ocenas, D., Skvarka, J., Zimnikoval, P., Murayama, H., and Ohtsuka, K.: 1995, *Earth Moon Planets* **68**, 479–486.
Suzuki, S.: 2003, in H. Yano, S. Abe and M. Yoshikawa (eds.), *Proceedings of the 2002 International Science Symposium on the Leonid Meteor Storms*. Tokyo Press CO., LTD., pp. 175–182.
Toda, M., Yamamoto, M.-Y., Higa, Y., and Watanabe, J.-I.: 2004, *Publ. Natl. Astron. Obs. Japan* **7**, 53–66.
Trigo-Rodriguez, J. M., Llorca, J., Borovička, J., and Fabregat, J.: 2004, *Meteoritics Plan. Sci.* **38**, 1283–1294.
Yamamoto, M.-Y., Toda, M., Higa, Y., Maeda, K., and Watanabe, J.-I.: 2005, *Earth, Moon, Planets*, this issue.